Supporting Information

Conformational Heterogeneity and the Affinity of Substrate Molecular Recognition by Cytochrome P450cam

Edward J. Basom,[a] Bryce A. Manifold,[a] and Megan C. Thielges[a]*

[a] Department of Chemistry, Indiana University, 800 East Kirkwood, Bloomington, Indiana 47405, United States
*Corresponding Author: thielges@indiana.edu

Contents

I. Supplemental Experimental Methods

P450cam Expression and Purification

Mutations for encoding Y96F or inserting an amber (TAG) codon were introduced into the P450cam sequence using standard site-directed mutagenesis (Stratagene QuikChange II kit, Agilent) and confirmed by sequencing (Genewiz). The sequence for all variants (WT, Y96F, and Y96CNF) also contains C334A that reduces protein aggregation, but has been shown to not affect the enzymatic activity.[1] The plasmid with the amber mutation at residue 96 was co-transformed with plasmid pUltraCNF, provided by Pete Schultz (Scripps Research Institute).[2] WT, Y96F, and Y96CNF P450cam variants were expressed in BL21(DE3) in Luria Broth at 37 °C while shaking at 250 rpm (200 rpm for Y96CNF). For Y96CNF, *p*-cyano-L-phenylalanine (ChemPep, Inc.) was added to 1 mM when the cultures reached OD_{600} = 0.2. Expression was induced at OD_{600} = 0.6 with 0.5 mM IPTG, at which time δ-aminolevulinic acid (Sigma Aldrich) and *d*-camphor (Sigma Aldrich) were added to 0.5 mM. Following expression for 14-16 hours, the cells were harvested by centrifugation, and cell pellets were stored at -20 °C.

Lysis and purification proceeded as previously reported (see SI of reference 3),[3] however Q media was substituted instead of DEAE for both columns. Pooled fractions from the second Q column were further purified on a 75 cm S100HR Sephacryl (GE Life Sciences) column in 50 mM potassium phosphate, pH 7, with 100 mM KCl and 1 mM *d*-camphor. Fractions with adequate purity (A_{390}/A_{280} > 1.3 for WT, A_{404}/A_{280} > 1.0 for Y96F, and A_{414}/A_{280} > 1.1 for Y96CNF) were combined and supplemented with 50% glycerol (w/v), flash frozen in $N_{2(l)}$, and stored at -80 °C.

Visible Spectroscopy

Visible absorption spectra (Figure S1) were collected with a Cary 300 UV-visible spectrophotometer. Spectra of P450cam variants in the free state and in complexes with each substrate were acquired at 1 μM protein in a 1 cm quartz cuvette, whereas samples in complexes with CO were acquired at 0.5-2 mM protein in FT IR sample cells (see the *FT IR Sample Preparation* section for the procedure to prepare the CO complexes). P450cam concentration was determined spectroscopically by the absorbance at either 417 nm (free state) or 390 nm (camphor complex) with the previously reported 100 $mM^{-1}cm^{-1}$ extinction coefficient, which is approximately valid for both states.[4] However, for complexes which exhibit a mixture of spin states, an extinction coefficient of 74.6 $mM^{-1}cm^{-1}$ at the isosbestic point (404 nm) was used.

Binding Assays

The K_D values for P450cam variants with camphor were determined by spectrophotometric titrations. P450cam samples were passed over a Sephadex G25 column (GE Life Sciences) in 50 mM TrisCl, pH 7.4, 20% glycerol, to remove camphor from the storage buffer, prior to equilibration into filtered and degassed 100 mM potassium phosphate, pH 7, 50 mM KCl, 20% glycerol. A solution of 5 mM *d*-camphor, prepared in the same phosphate buffer,

was titrated into a sample of 1 μM protein. Visible absorbance difference spectra were collected with a baseline to the initial sample. All absorbance values were adjusted for dilution of the protein assuming a linear dependence on concentration. The difference in absorbance at 420 nm (ΔA_{420}) relative to the substrate-free sample was plotted as a function of the camphor concentration and fit to equation 1, derived from the expression for the equilibrium between a protein (P), ligand (L), and the complex (PL), where P_t is the total protein concentration, L_t is the total ligand concentration, and ΔA_{420}^{max} is the maximum observed absorbance at 420 nm.

$$\frac{\Delta A_{420}}{\Delta A_{420}^{max}} = \frac{(K_D+P_t+L_t)-\sqrt{(-K_D-P_t-L_t)^2-4P_tL_t}}{2P_t} \quad (1)$$

To determine K_D values for the P450cam variants with isoborneol (which is racemic, but a pure diastereomer) and camphane, a 0.6 μM protein sample (equilibrated as above) was split into two samples: one of which was diluted two-fold with buffer (filtered and degassed 100 mM potassium phosphate, pH 7, 50 mM KCl, 20% glycerol) whereas the other was diluted two-fold in the same buffer but containing substrate (2 mM isoborneol or 100 μM camphane). Therefore, the two samples both contained 0.3 μM protein, but only one contained the substrate (1 mM isoborneol or 50 μM camphane). A visible absorbance baseline was acquired to the substrate-free sample with a carefully characterized volume in order to perform a constant-volume titration. The substrate-bound sample was exchanged step-wise into the substrate-free sample following equation 2, in which the volume to remove from the sample in the cuvette and replace with the same volume of substrate-bound sample at each step (V_{ex}) was calculated from the current concentration of substrate in the sample at that step ($[S]_i$), the final concentration desired for that step ($[S]_f$), the total volume to be maintained following the exchange (V_{tot}), and the concentration of substrate in the bound sample ($[S]_s$).

$$V_{ex} = \frac{[S]_f \cdot V_{tot} - [S]_i \cdot V_{tot}}{[S]_s - [S]_i} \quad (2)$$

Visible absorbance difference spectra were collected after each step, and the K_D was calculated from the data in the same way as above, however it was necessary to extrapolate the fit for camphane K_Ds due to the low solubility of camphane.

FT IR Sample Preparation

The camphor complex was prepared by equilibration into 100 mM potassium phosphate, pH 7, 50 mM KCl, 20% glycerol, and 5 mM *d*-camphor. With the exception of the camphor complex, all other P450cam samples used in IR experiments were passed over a 10 cm Sephadex G25 column (GE Life Sciences) in 50 mM TrisCl, pH 7.4, 20% glycerol, to remove camphor from the storage buffer. The substrate-free protein was equilibrated into 100 mM potassium phosphate, pH 7, 50 mM KCl, 20% glycerol by three rounds of 10-fold concentration and dilution, then concentrated to 0.5-2 mM. The camphane (Apollo Scientific) and isoborneol (Santa Cruz Biotech) complexes were prepared from the substrate-free P450cam by addition of sufficient substrate from an ethanol stock solution to ensure less than 5% substrate-free protein in

the sample. All samples with camphane and isoborneol were left to gently rock overnight at 4 °C to ensure dissolution of the substrate. In all cases, there was no more than 4% ethanol in the sample; higher concentrations of ethanol were found to coincide with a small (~5%) quantity of inactive enzyme.

To prepare the P450cam-carbon monoxide (P450camCO) complex, 8 μL aliquots of the concentrated protein samples were placed in PCR tubes sealed with rubber septa. The headspace of each sample was gently purged under $Ar_{(g)}$ and $CO_{(g)}$ for several minutes, followed by reduction with 10 equivalents of sodium dithionite. The headspace was again purged with $CO_{(g)}$ for several minutes and the tube was agitated intermittently in order to bind CO. The CO-bound samples were loaded between CaF_2 windows (1 mm thick) with a 38 μm Teflon spacer. Visible spectra of all samples were acquired before and after FT IR data collection to ensure the absence of a peak at 420 nm, which is indicative of the inactive enzyme.[5] All complexes displayed the expected band at 446 nm when bound to CO (Figure S2).

II. Supplemental Discussion

Spin States of P450cam Complexes

The percentages of high-spin heme for each of our P450cam complexes determined from the visible spectra are reported in Table S1. In the complex with camphor (and sufficient potassium), it is well established that wild-type P450cam exists in essentially 100% high-spin state,[4] and for simplicity, we treated the spin-state as such herein, however it should be noted that a small amount of low-spin heme (~5%) is present even in the camphor-bound spectrum. Changes in P450cam spin state equilibrium upon substrate binding have long been known to be a prerequisite for thermodynamics of the initial reduction of the heme (Fe^{3+} to Fe^{2+}).[6] Predominance of the high-spin state is generally attributed to exclusion of active site water upon camphor binding, which leads to a pentacoordinate heme iron atom.[6,7] However, alternative mechanisms for explaining the spin state have been proposed in light of crystal structures which are inconsistent with the heme coordination argument,[8] and evidence from vibrational coherence spectroscopy suggest a role for the heme porphyrin conformation in determining the spin state equilibrium.[9] We do not observe any clear pattern between P450cam affinity for a given substrate and the population of high-spin heme; similarly, previous studies have noted that population of high-spin heme is not a reliable indicator of P450cam affinity for a substrate.[10-12]

Evaluation of Fits to IR Spectra

First, the CN stretches for the Y96CNF complexes were analyzed to determine the maximum frequency (ν_{max}), average frequency at half-maximum ($\nu_{half\text{-}max}$), and full-width at half-maximum (FWHM). These parameters can be determined without fitting the band shapes, thus any uncertainty in their values is only due to uncertainty from baseline subtraction and experimental limitations (Table S3). Each spectrum was then fit to a single or sum of two Gaussian functions (Tables S4 and S5). The significance of inclusion of the second component was evaluated by F-tests (Table S6).[13] For six of the eight spectra, the two-component fit was favored. One of the exceptions was the spectrum for substrate-free Y96CNF, for which the inclusion of a second component marginally but not significantly improved the fit based on F-tests (Table S6). Additionally, for the camphor complex, the single-component fit was decidedly superior. This is also the case if the frequency of one of the bands is fixed (e.g. at 2234 cm^{-1}, Table S7). In addition, the uncertainties in many parameters for the two-component fits were large (note however that the parameters obtained without fitting, Table S3, were highly reproducible). Thus, the fitting statistics do not support two components in the spectra for the camphor complex. On the other hand, it is notable that in all cases the fits to the averaged data sets (Table S8 and Figure S7) correspond well to the average of the fits to the individual data sets (Tables S4 and S5).

As for the CN spectra, the CO spectra were fit to one or a sum of Gaussian functions, and the significance of inclusion of additional components was evaluated by F-tests. Alternate fits were also evaluated for Y96CNF-CO to investigate possible models for the relative population of states that are consistent with both the CN and CO spectral data. Inclusion of a second, higher frequency band significantly improves the fits of the CO spectra of Y96CNF-CO-camphane and Y96CNF-CO-isoborneol complexes (Table S10), but for both the relative integrated areas of the

additional bands are negligible (2-3%) (Table S9). In contrast, the CO spectrum for substrate-free Y96CNF-CO is best fit with two bands. To evaluate if this spectrum could be modeled with the three bands determined from the fit of the CO spectra for the camphor complex, we attempted to fit the spectra to three-components with all three center frequencies fixed correspondingly; however, the obtained fit was not reasonable. If the lowest frequency component solely is fixed (to 1945.6 cm^{-1}), the resultant fit is acceptable, although not significantly improved by the additional component. The results also give a band at intermediate frequency that is significantly blue-shifted from the corresponding band at intermediate frequency for the camphor complex (Table S9). Similarly, for substrate-free Y96F-CO, if the lowest frequency band is fixed to that found for the camphor complex (1945.7 cm^{-1}), the fit is modestly improved, but the relative integrated area of the band is only 1%. Finally, fitting the CO spectrum of the substrate-free Y96CNF-CO with frequencies unfixed yields bands at ~1953, 1957, and 1964 cm^{-1} (Table S9); the lower two frequencies do not match either obtained for the camphor complex. Altogether, the CO stretch parameters reported in Table 2 (main text) represent the values in which we have the most confidence.

Model for population of multiple states to account for CN and CO bands of Y96CNF-CO

We start with a model consisting of a minimum of three states to account for the three distinct CO bands for the camphor complex. For clarity in our discussion, the lowest, middle, and highest frequency CO bands are assigned to states referred to as S1, S2, and S3, respectively. A relatively narrow band at ~1964 cm^{-1}, nearly the same frequency as the S3 band for the camphor complex, appears in the CO spectra of the substrate-free protein, and so we assigned this band to S3. Since the relative bands areas for the CN and CO components for the substrate-free protein exactly match, we assign the CN band at 2232.6 cm^{-1} to S3. Now reconsidering the camphor complex, to account for the relative CN and CO band areas, the state reflected by the high frequency CN band (2235.3 cm^{-1}) can reasonably be assigned to overlapping features of S1 combined with either S2 or S3. This implies that the minor CN band corresponds to states S2 or S3. Because S3 has been assigned to the CN band at 2232.6 cm^{-1} in the substrate-free protein, for the camphor complex we think it more likely that the S3 state contributes to the unresolved features underlying the band at 2235.3 cm^{-1} than reflects the band at 2227.8 cm^{-1}. Thus, for the camphor complex, the CN band at 2235.3 cm^{-1} is assigned to a combination of S1 and S3, while the CN band at 2227.8 cm^{-1} is assigned to S2. For the camphane and isoborneol complexes, the CO spectra are well fit by a single band, but the CN spectra are best fit by two (Table S6). As the CO band at 1964.2 cm^{-1} corresponding to population of S3 is clearly absent from the CO spectra for isoborneol and camphane complexes, the two CN bands are assigned to states S1 and S2. To be consistent with the higher frequency CN band of the camphor complex corresponding to the dominant state, the high and low frequency CN bands for the camphane and isoborneol are assigned to the S1 and S2 states, respectively. Since the CO bands assigned to S1 and S2 for the camphor complex are close in frequency, this assignment also is consistent with their being unresolved in the CO spectra for the camphane and isoborneol complexes. In addition, the CN

band for all states assigned to S2 in the substrate complexes show similarly low frequency, and we think it reasonable that the second CN band for the substrate-free complex also corresponds to the S2 state. Altogether, the relative populations of the three states in absence or presence of the different substrates from this model are listed in Table S11.

Based on these assignments, we then extended the model to the conformational populations for Y96CNF in the absence of CO (Table S12). Since the frequencies of the bands for the isoborneol and camphane complexes are independent of CO, the associated states likely correspond, and so are assigned to S1 and S2. The spectra for the substrate-free and camphor complex are well fit by a single band, so they can be assigned to 100% one state. The camphor complex is assigned to S1, in agreement with those most highly populated for the isoborneol/camphane complexes. The substrate-free state is assigned that mostly highly populated in the CO complex. For the case that one assumes that the spectrum for the camphor complex is two-component, the fit yields one band at the same frequency as found for the isoborneol/camphane complexes (Table S5). We thus assign this band to S2 and the lower frequency band to S1 to generate the model for conformational populations given in Table S13.

III. Supplemental Figures and Tables

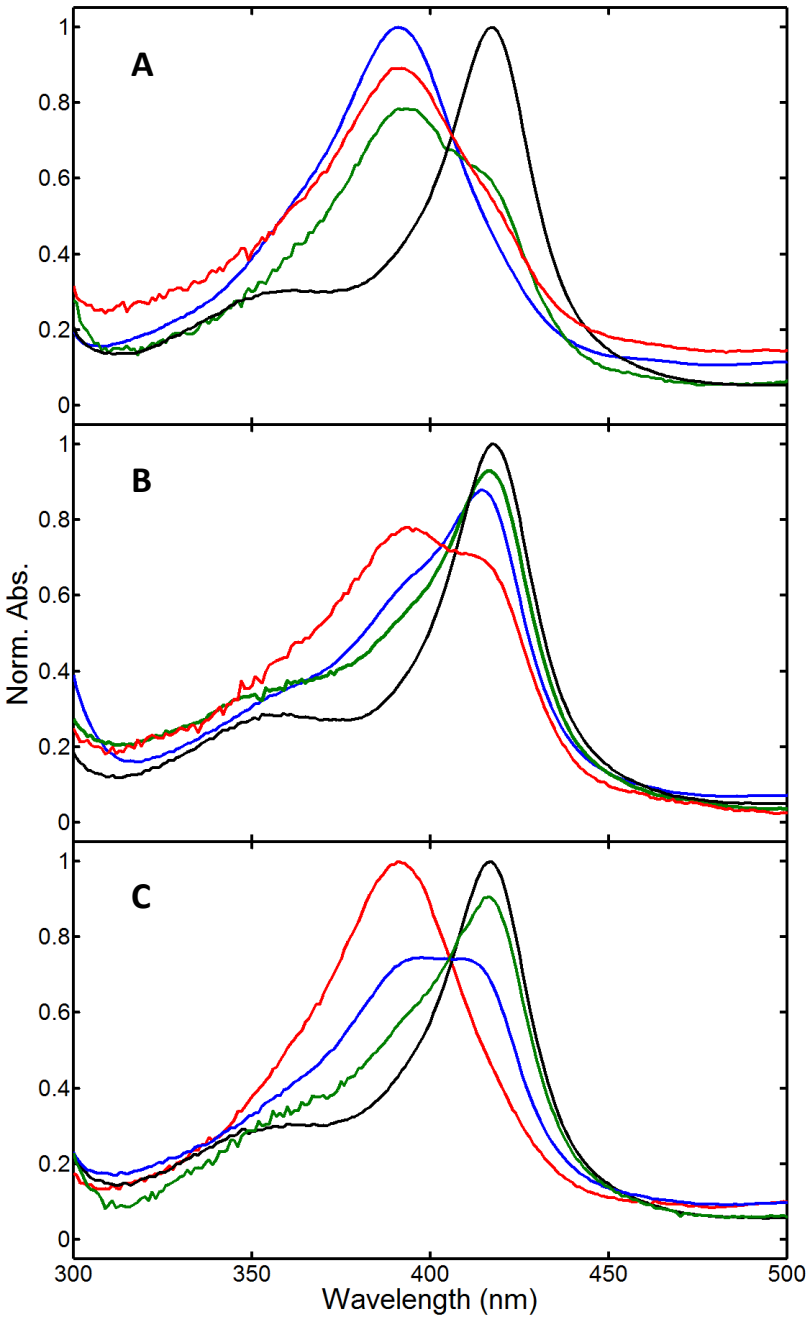

Figure S1. Representative visible absorbance spectra for (A) wild-type, (B) Y96CNF, and (C) Y96F P450cam in complexes with camphor (blue), isoborneol (green), and camphane (red), as well as the substrate-free form (black).

Table S1. Spin State Populations of P450cam Complexes

Variant	Substrate	High-Spin Population (%)
All	free	0
WT	camphor	100
WT	isoborneol	68 ± 2
WT	camphane	86 ± 2
Y96CNF	camphor	33 ± 1
Y96CNF	isoborneol	14 ± 1
Y96CNF	camphane	72 ± 14
Y96F	camphor	55 ± 3
Y96F	isoborneol	28 ± 4
Y96F	camphane	98 ± 2

Table S2. Interaction Energies from Thermodynamic Cycles

Variant	Substrate	ΔG_{int} (kcal/mol)
WT	camphor	-0.7 ± 0.5
WT	isoborneol	1.0 ± 0.4
Y96CNF	camphor	0.3 ± 0.5
Y96CNF	isoborneol	1.2 ± 0.4

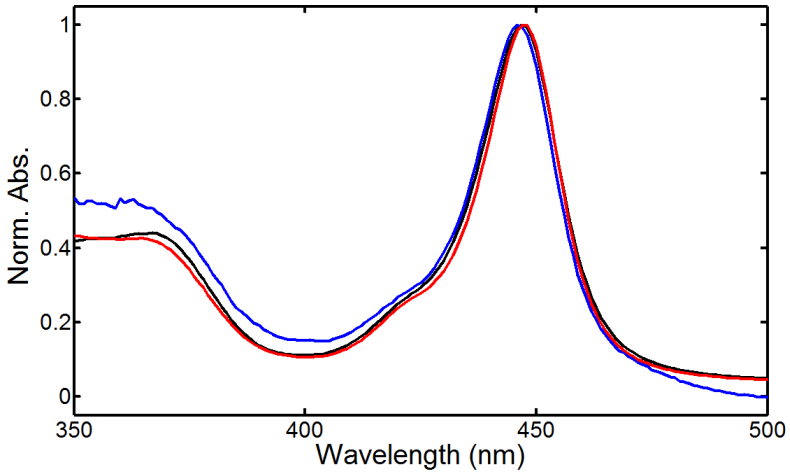

Figure S2. Representative visible absorbance spectra for CO-bound wild-type (black), Y96F (blue), and Y96CNF (red) P450cam.

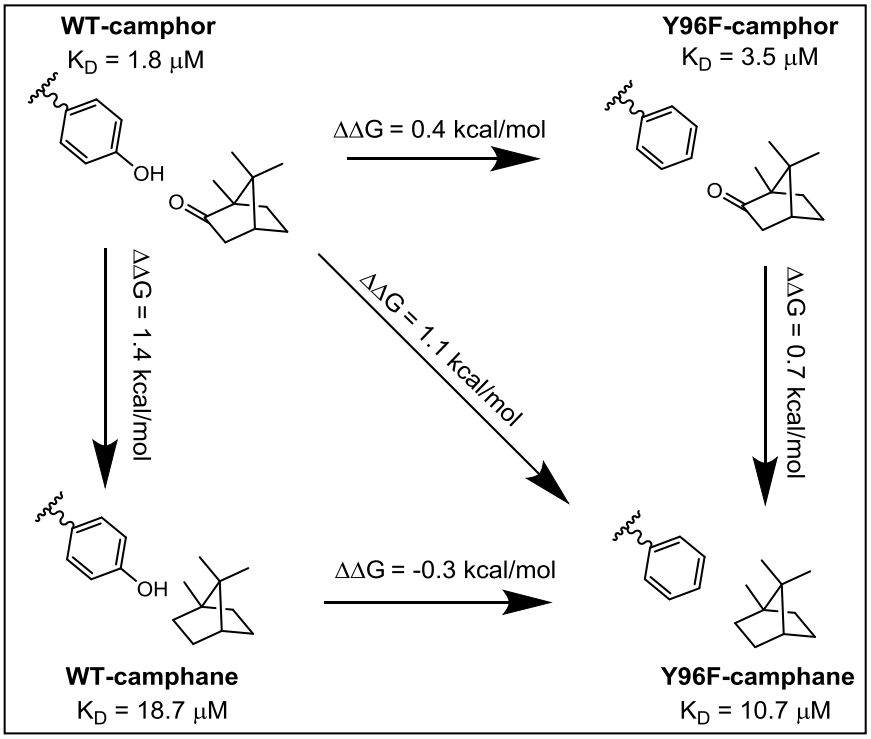

Figure S3. Thermodynamic Cycle for WT P450cam with Camphor

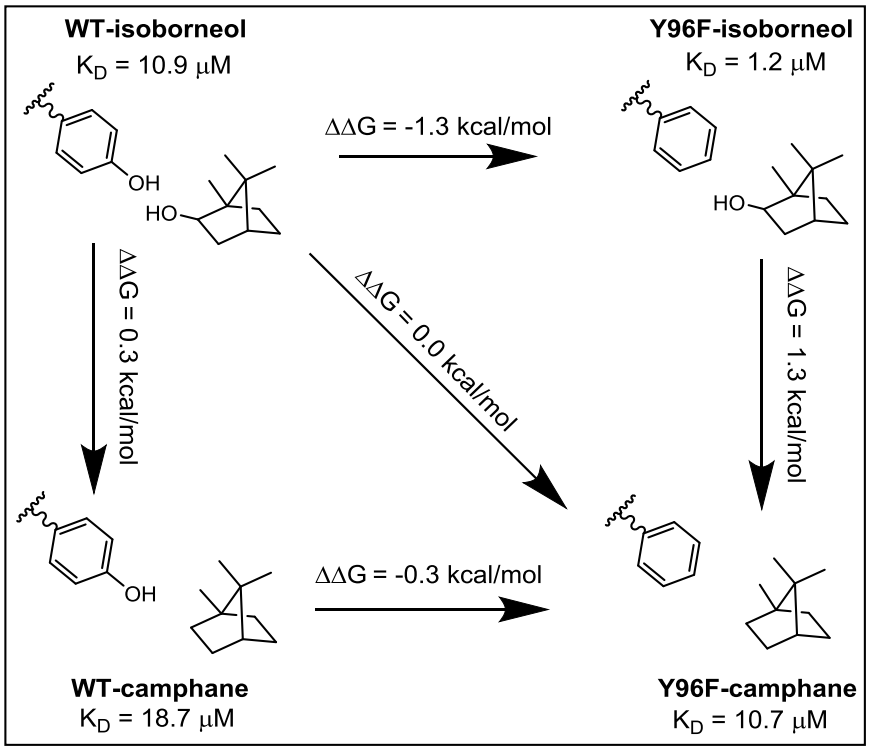

Figure S4. Thermodynamic Cycle for WT P450cam with Isoborneol

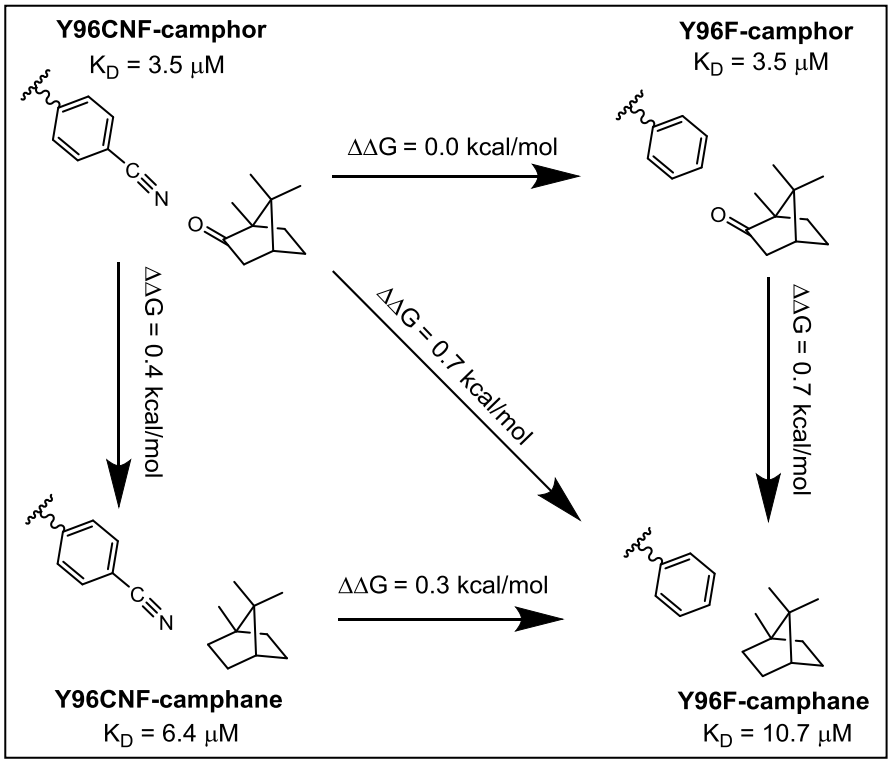

Figure S5. Thermodynamic Cycle for Y96CNF P450cam with Camphor

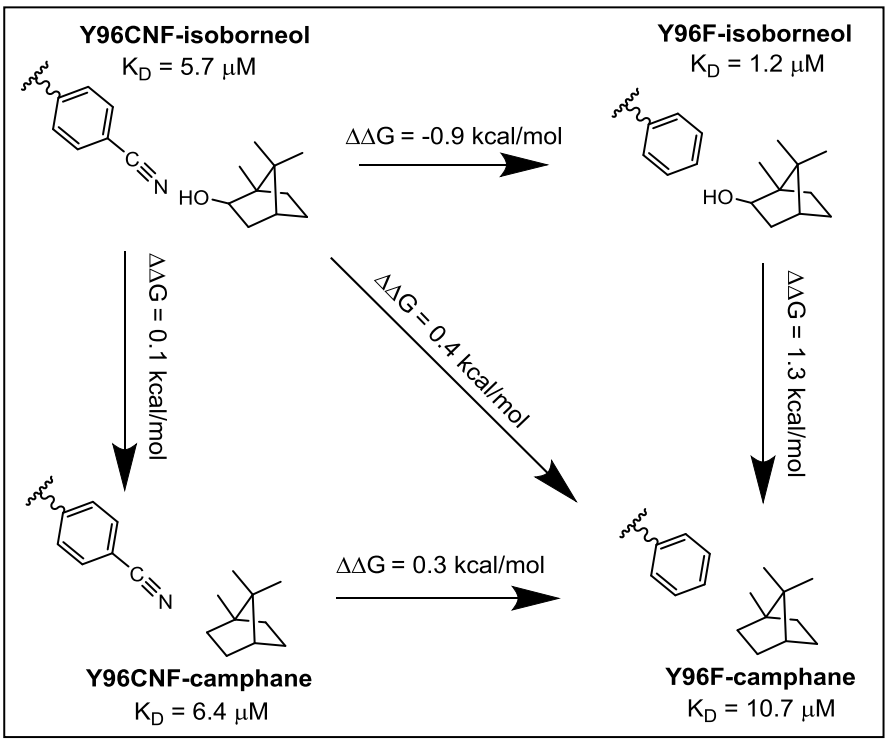

Figure S6. Thermodynamic Cycle for Y96CNF P450cam with Isoborneol

Table S3. Parameters of CN Spectra for Y96CNF

Ligand/Substrate	ν_{max} (cm^{-1})	$\nu_{half\text{-}max}$ (cm^{-1})	FWHM (cm^{-1})
none	2232.1 ± 0.1	2232.4 ± 0.1	10.9 ± 0.2
camphor	2233.0 ± 0.1	2232.9 ± 0.2	12.0 ± 0.5
isoborneol	2232.2 ± 0.7	2232.4 ± 0.3	11.4 ± 0.3
camphane	2233.6 ± 0.2	2233.3 ± 0.3	8.0 ± 0.5
CO	2228.1 ± 0.02	2230.2 ± 0.1	10.4 ± 0.2
CO/camphor	2235.4 ± 0.03	2234.8 ± 0.1	9.8 ± 0.2
CO/isoborneol	2233.7 ± 0.1	2233.5 ± 0.1	12.1 ± 0.1
CO/camphane	2233.7 ± 0.3	2233.3 ± 0.3	10.7 ± 0.4

Table S4. Parameters from Single-Component Fits of CN Spectra for Y96CNF

Ligand/Substrate	ν_{CN} (cm^{-1})	FWHM (cm^{-1})
none	2232.5 ± 0.2	11.2 ± 0.7
camphor	2232.9 ± 0.2	12.1 ± 0.5
isoborneol	2232.6 ± 0.4	10.6 ± 0.3
camphane	2233.5 ± 0.3	7.6 ± 0.7
CO	2230.3 ± 0.2	10.6 ± 0.2
CO/camphor	2234.7 ± 0.1	10.3 ± 0.2
CO/isoborneol	2233.5 ± 0.1	12.0 ± 0.1
CO/camphane	2233.4 ± 0.1	10.3 ± 0.2

Table S5. Parameters from Two-Component Fits of CN Spectra for Y96CNF

Ligand/Substrate	ν_{CN} (cm^{-1})	FWHM (cm^{-1})	Rel. Area (%)
none	2230.4 ± 0.3	8.5 ± 0.5	52 ± 8
	2235.1 ± 0.6	9.8 ± 0.2	48 ± 8
camphor	2232.4 ± 0.3	10.5 ± 0.3	47 ± 16
	2233.8 ± 1.2	14.7 ± 2.3	53 ± 16
isoborneol	2228.9 ± 0.2	6.6 ± 0.7	32 ± 8
	2234.2 ± 0.2	8.8 ± 0.5	68 ± 8
camphane	2229.6 ± 0.3	5.0 ± 0.4	15 ± 2
	2234.0 ± 0.2	6.8 ± 0.4	85 ± 2
CO	2227.2 ± 0.1	5.7 ± 0.2	42 ± 7
	2232.6 ± 0.4	8.4 ± 0.7	58 ± 7
CO/camphor	2227.8 ± 0.1	6.2 ± 0.1	12 ± 1
	2235.3 ± 0.05	8.9 ± 0.1	88 ± 1
CO/isoborneol	2228.0 ± 0.4	8.3 ± 1.0	9 ± 4
	2234.0 ± 0.3	11.3 ± 0.3	91 ± 4
CO/camphane	2228.0 ± 0.1	6.1 ± 0.2	10 ± 0.5
	2233.9 ± 0.2	9.5 ± 0.3	90 ± 0.5

Table S6. F-tests for Fits to CN Spectra for Y96CNF

Ligand/Substrate	Number of Components	SSE[a]	DOF[b]	F_{exp}[c]	$F_{critical}$ ($\alpha = 0.1$)	$F_{critical}$ ($\alpha = 0.01$)
none	1	0.00185	49	0.25	2.23	4.31
	2	0.00182	46			
camphor	1	0.00153	49	-7.09	2.23	4.31
	2	0.00284	46			
	2 (fixed)*	0.00308	47	-11.83	2.23	4.31
isoborneol	1	0.00982	23	17.44	2.38	4.94
	2	0.00272	20			
camphane	1	0.01244	23	7.74	2.38	4.94
	2	0.00575	20			
CO	1	0.01024	49	56.04	2.23	4.31
	2	0.00220	46			
CO/camphor	1	0.00381	49	43.09	2.23	4.31
	2	0.00100	46			
CO/isoborneol	1	0.00919	33	11.45	2.28	4.51
	2	0.00429	30			
CO/camphane	1	0.02857	26	30.95	2.34	4.76
	2	0.00567	23			

[a]Sum of squared errors of prediction [b]Degrees of freedom
[c]F-value (F_{exp}) = $[(SSE_1-SSE_2)/(DOF_1-DOF_2)]/(SSE_2/DOF_2)$
*See Table S7

Table S7. Parameters from Fit of CN Spectra for Y96CNF Camphor Complex with Fixed Frequency

ν_{CN} (cm^{-1})	FWHM (cm^{-1})	Rel. Area (%)
2232.3 ± 0.4	10.7 ± 0.9	61 ± 28
2234.0 (fixed)	14.8 ± 2.8	39 ± 28

Table S8. Parameters from Fits of Averaged CN Spectra for Y96CNF

Ligand/Substrate	Number of Components	ν_{CN} (cm^{-1})	FWHM (cm^{-1})	Rel. Area (%)
none	1	2232.5	11.2	
	2	2230.5	8.7	42
		2234.5	11.0	58
camphor	1	2232.9	12.2	
	2	2232.4	10.3	50
		2233.7	14.8	50
isoborneol	1	2232.5	10.7	
	2	2228.8	6.5	30
		2234.2	8.9	70
camphane	1	2233.4	7.8	
	2	2229.7	5.1	16
		2234.0	6.8	84
CO	1	2230.3	10.6	
	2	2227.2	5.6	40
		2232.5	8.5	60
CO/camphor	1	2234.7	10.3	
	2	2227.7	6.2	12
		2235.3	9.0	88
CO/isoborneol	1	2233.5	12.0	
	2	2227.5	8.0	6
		2233.9	11.5	94
CO/camphane	1	2233.3	10.5	
	2	2227.9	6.1	10
		2233.9	9.5	90

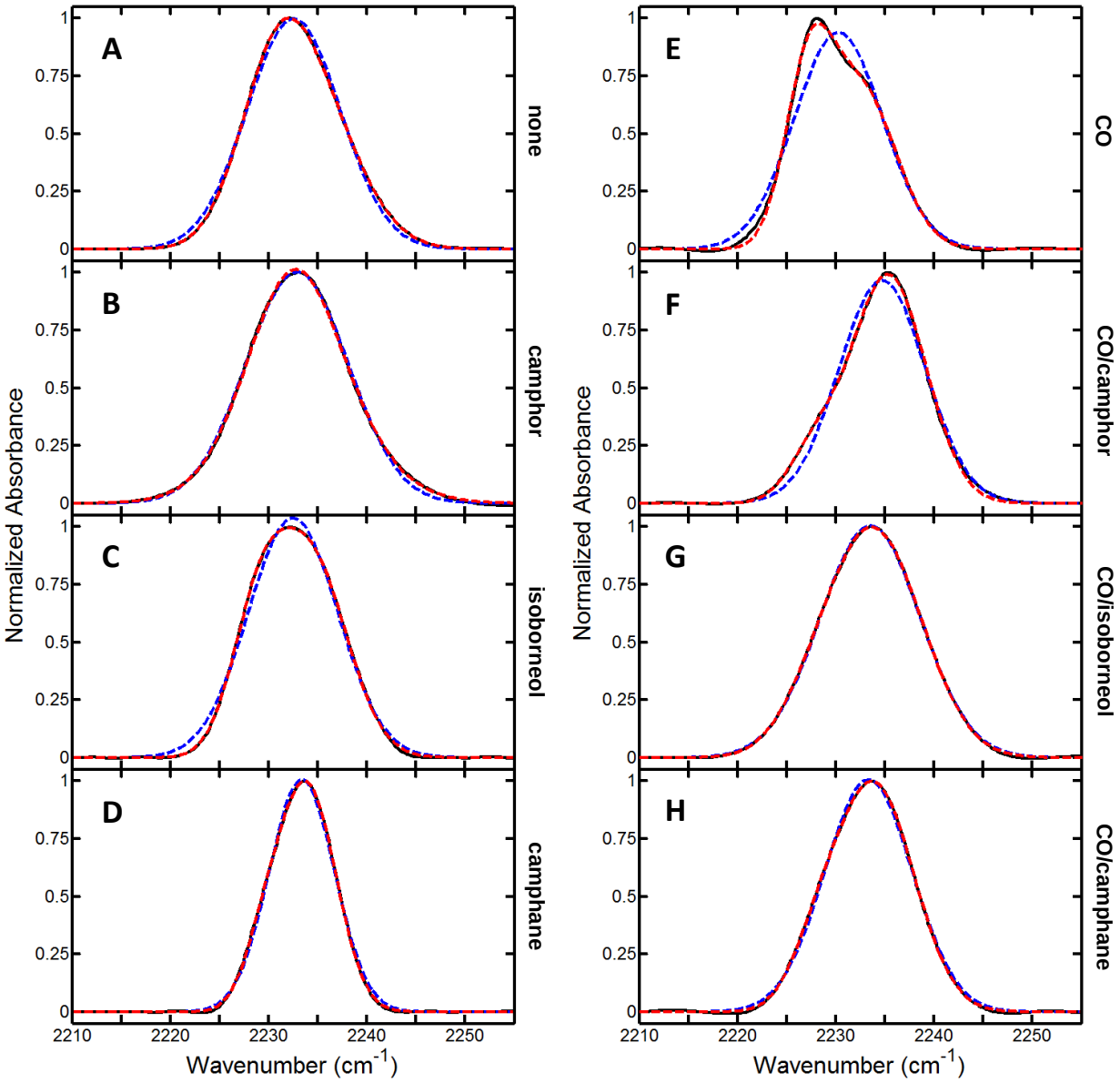

Figure S7. Comparison of single (blue dashed lines) and two-component (red dashed lines) Gaussian fits of CN spectra for Y96CNF complexes. Black lines are the averaged data of at least three unique trials. Left panels (A-D) are spectra without CO, right panels (E-H) include heme-bound CO. Top row: substrate-free. Second row: camphor-bound. Third row: isoborneol-bound. Bottom row: camphane-bound.

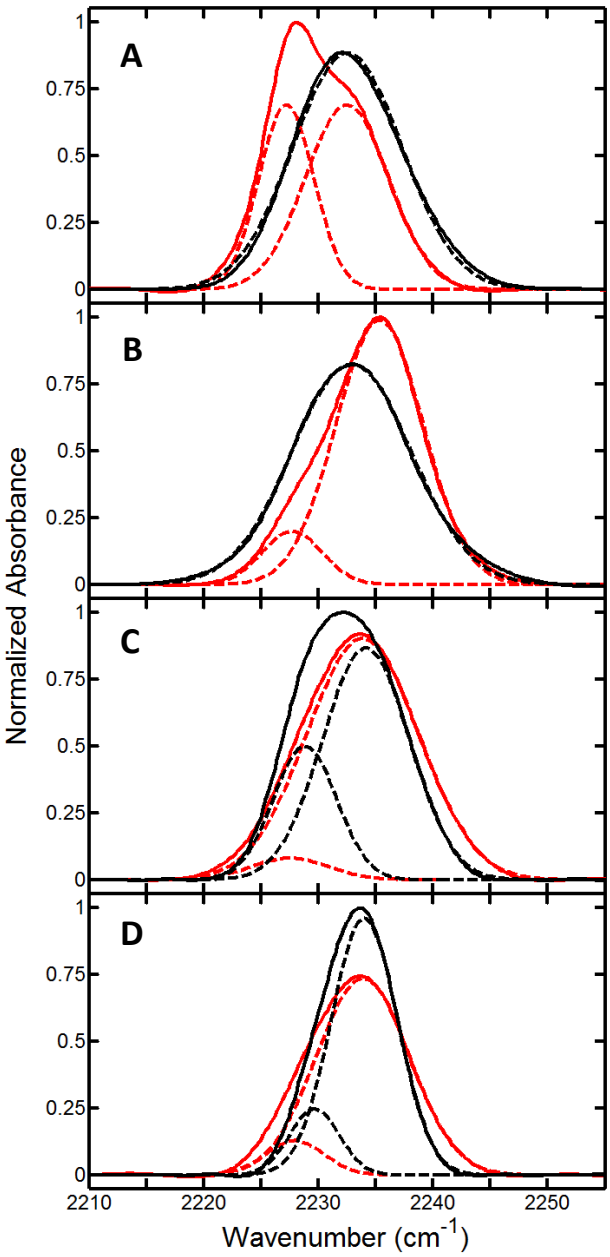

Figure S8. CN spectra shown in Figure 5 (main text) including component bands from fits (dashed lines) for Y96CNF in the absence (black) and presence (red) of CO for the substrate-free state (A), and complexes with camphor (B), isoborneol (C), and camphane (D). All spectra are normalized relative to the integrated areas under the other spectrum in each panel.

Table S9. Parameters for Alternative Fits to Select CO Spectra

Variant	Ligand/Substrate	ν_{CO} (cm^{-1})	FWHM (cm^{-1})	Rel. Area (%)
		Two-Component Fits		
Y96CNF	CO/isoborneol	1949.8 ± 0.03	14.1 ± 0.7	97 ± 1
		1965.1 ± 0.7	6.5 ± 1.1	3 ± 1
Y96CNF	CO/camphane	1951.5 ± 0.1	10.8 ± 0.2	98 ± 0.2
		1962.6 ± 1.1	7.4 ± 0.4	2 ± 0.2
		Three-Component Fits with a Fixed Frequency		
Y96F	CO	1945.7 (fixed)	5.4 ± 2.0	1 ± 1
		1957.4 ± 1.1	13.5 ± 0.7	45 ± 6
		1963.1 ± 0.07	8.7 ± 0.1	54 ± 7
Y96CNF	CO	1945.6 (fixed)	16.4 ± 0.9	16 ± 2
		1959.6 ± 0.2	16.1 ± 0.1	39 ± 1
		1964.5 ± 0.03	8.6 ± 0.05	45 ± 1
		Three-Component Fits		
Y96CNF	CO	1952.8 ± 0.7	22.7 ± 0.5	39 ± 1
		1957.1 ± 0.2	7.5 ± 0.9	5 ± 1
		1964.4 ± 0.03	9.0 ± 0.1	56 ± 1

Table S10. F-tests for Alternative Fits to Select CO Spectra

Variant	Ligand/Substrate	Number of Components	SSE[a]	DOF[b]	F_{exp}[c]	$F_{critical}$ ($\alpha = 0.1$)	$F_{critical}$ ($\alpha = 0.01$)
Y96CNF	CO/isoborneol	1	0.04294	49	5.84	2.20	4.20
		2	0.03110	46			
Y96CNF	CO/camphane	1	0.02148	49	10.48	2.20	4.20
		2	0.01276	46			
Y96F	CO	2	0.02191	46	2.76	2.23	4.31
		3 (fixed)	0.01837	44			
Y96CNF	CO	2	0.00182	46			
		3 (fixed)	0.00239	44	-3.42	2.23	4.31
		3	0.00359	43	-7.06	2.23	4.31

[a]Sum of squared errors of prediction [b]Degrees of freedom
[c]F-value (F_{exp}) = $[(SSE_1-SSE_2)/(DOF_1-DOF_2)]/(SSE_2/DOF_2)$

Table S11. Populations of states for CO complexes from combined CO/CN spectral analysis

	free	camphor	isoborneol	camphane
S1		82	91	90
S2	42	9	9	10
S3	58	9		

Table S12. Populations of states in absence of CO – spectrum for camphor complex modeled with one component

	free	camphor	isoborneol	camphane
S1		100	68	85
S2			32	15
S3	100			

Table S13. Populations of states in absence of CO – spectrum for camphor complex modeled with two components

	free	camphor	isoborneol	camphane
S1		47	68	85
S2		53	32	15
S3	100			

IV. References

(1) Nickerson, D. P., and Wong, L.-L. (1997) The dimerization of *Pseudomonas putida* cytochrome P450cam: practical consequences and engineering of a monomeric enzyme, *Protein Eng. 10*, 1357-1361.

(2) Chatterjee, A., Sun, S. B., Furman, J. L., Xiao, H., and Schultz, P. G. (2013) A Versatile Platform for Single- and Multiple-Unnatural Amino Acid Mutagenesis in *Escherichia coli*, *Biochemistry 52*, 1828-1837.

(3) Basom, E. J., Spearman, J. W., and Thielges, M. C. (2015) Conformational Landscape and the Selectivity of Cytochrome P450cam, *J. Phys. Chem. B 119*, 6620-6627.

(4) Peterson, J. A. (1971) Camphor Binding by Pseudomonas Putida Cytochrome P-450, *Arch. Biochem. Biophys. 144*, 678-693.

(5) Yu, C.-A., and Gunsalus, I. C. (1974) Cytochrome P-450cam II. Interconversion with P-420, *J. Biol. Chem. 249*, 102-106.

(6) Sligar, S. G. (1976) Coupling of Spin, Substrate, and Redox Equilibria in Cytochrome P450, *Biochemistry 15*, 5399-5406.

(7) Wells, A. V., Li, P., and Champion, P. M. (1992) Resonance Raman Investigations of *Escherichia coli*-Expressed *Pseudomonas putida* Cytochrome P450 and P420, *Biochemistry 31*, 4384-4393.

(8) Raag, R., and Poulos, T. L. (1989) The Structural Basis for Substrate-Induced Changes in Redox Potential and Spin Equilibrium in Cytochrome P-450cam, *Biochemistry 28*, 917-922.

(9) Karunakaran, V., Denisov, I., Sligar, S. G., and Champion, P. M. (2011) Investigation of the Low Frequency Dynamics of Heme Proteins: Native and Mutant Cytochrome P450(cam) and Redox Partner Complexes, *J. Phys. Chem. B 115*, 5665-5677.

(10) Colthart, A. M., Tietz, D. R., Ni, Y., Friedman, J. L., Dang, M., and Pochapsky, T. C. (2016) Detection of substrate-dependent conformational changes in the P450 fold by nuclear magnetic resonance, *Sci. Rep. 6*, 22035.

(11) French, K. J., Rock, D. A., Rock, D. A., Manchester, J. I., Goldstein, B. M., and Jones, J. P. (2002) Active Site Mutations of Cytochrome P450cam Alter the Binding, Coupling, and Oxidation of the Foreign Substrates (R)- and (S)-2-Ethylhexanol, *Arch. Biochem. Biophys. 398*, 188-197.

(12) Bell, S. G., Chen, X., Sowden, R. J., Xu, F., Williams, J. N., Wong, L.-L., and Rao, Z. (2003) Molecular Recognition in (+)-α-Pinene Oxidation by Cytochrome P450cam, *J. Am. Chem. Soc. 125*, 705-714.

(13) Graham, R. C. (1993) *Data Analysis for the Chemical Sciences: A Guide to Statistical Techniques*, VCH Publishers, New York.